Micro-hydration of the $MgNO_3^+$ cation in the gas phase

Barbara Jagoda-Cwiklik, Pavel Jungwirth,[*] Lubomír Rulíšek, Petr Milko, Jana Roithová, Joël Lemaire, Philippe Maitre, Jean Michel Ortega, and Detlef Schröder[*]

Abstract: Coordination complexes of the magnesium-nitrate cation with water $[MgNO_3(H_2O)_n]^+$ up to n = 7 are investigated by experiment and theory. The fragmentation patterns of $[MgNO_3(H_2O)_n]^+$ clusters generated via electrospray ionization indicate a considerable change in stability between n = 3 and 4. Further, ion/molecule reactions of mass-selected $[MgNO_3(H_2O)_n]^+$ cations with D_2O reveal the occurrence of consecutive replacement of water ligands by heavy water, and in this respect the complexes with n = 4 and 5 are somewhat more reactive than their smaller homologs with n = 1 - 3 as well as the larger clusters with n = 6 and 7. For the latter two ions, experimental evidence as well as theory suggests the existence of isomers, such as complexes with monodentate nitrato ligands as well as solvent-separated ion pairs with a common solvation shell. The reactions observed and the ion thermochemistry are discussed in the context of ab initio calculations, which also reveal the structures of the various hydrated cation complexes.

Keywords: • electrospray ionization • hydration • magnesium cation • mass spectrometry • solvation • water clusters

[*] Dr. B. Jagoda-Cwiklik, Prof. P. Jungwirth
Institute of Organic Chemistry and Biochemistry, Center for Biomolecules and Complex Molecular Systems, Academy of Sciences of the Czech Republic, Flemingovo nám. 2, 16610 Prague 6, (Czech Republic)
Fax: int. code + (420) 220 410 320, e-mail: pavel.jungwirth@uochb.cas.cz
Ing. P. Milko, Dr. J. Roithová, Dr. L. Rulíšek, Dr. D. Schröder
Institute of Organic Chemistry and Biochemistry, Academy of Sciences of the Czech Republic, Flemingovo nám. 2, 16610 Prague 6 (Czech Republic)
Fax: int. code + (420) 220 183 117, e-mail: detlef.schroeder@uochb.cas.cz
Dr. J. Roithová
Department of Organic Chemistry, Charles University, Hlavova 8, 12843 Prague 2 (Czech Republic)
Dr. J. Lemaire, Dr. P. Maitre, Dr. J. M. Ortega
Laboratoire Chimie-Physique, UMR8000, Université Paris-Sud, CNRS, Faculté des sciences, Bât. 350, 91405 Orsay Cedex (France)

Introduction

Solvation of ions is of outmost importance for understanding the behavior of metals in condensed media.[1-3] On a molecular level, however, ion solvation is difficult to study in the condensed phase, and in this respect investigations of mass-selected ions in the gas-phase can provide valuable complementary information.[4] While clusters of alkali and alkali earth cations with water molecules have been subject of numerous investigations, much less is known about micro-hydration of complexes of a divalent cation (or anion) with a monovalent anion (or cation). Such systems still bear a full charge and can, therefore, be size-selected and spectroscopically characterized by experimental methods developed for charged clusters. At the same time, these systems allow for examination of micro-hydration of molecular ions M^{z+} bearing a counterion X^- with the possibility of a transition between contact- and solvent-separated ion pairs (equation 1).

$$\underset{\text{contact ion pair}}{[(H_2O)_nM^{z+}\bullet X^-]} \rightarrow \underset{\text{solvent-separated ion pair}}{[(H_2O)_{n-m}M^{z+}]\bullet[(H_2O)_mX^-]} \qquad \text{(eq. 1)}$$

Such situations, which frequently occur in bulk solution can be studied in much greater molecular detail in clusters employing both spectroscopic and computational tools. As an example, the structures and energetics of $[NaSO_4(H_2O)_n]^-$ clusters, where both contact and solvent-separated sodium-sulfate ion pairs could be identified and have been characterized by means of ab initio calculations and probed by photoelectron spectroscopy.[2]

Magnesium has recently received particular attention due to its divalent character,[5] and particularly the gas-phase chemistry of $[Mg(H_2O)_n]^{2+}$ dications has been studied in quite some detail by theory and experiment.[6-15] Further, magnesium ions have been discussed in the context of the possible formation of contact ion pairs in aqueous solution.[16-18] Nitrate is of particular interest as a counterion, because it can either bind as a mono- or bidentate ligand,[19,20] but as a weakly coordinating anion, it may also promote the formation of ion pairs. Further, the structures and vibrational spectra of a large number of nitrato complexes have been characterized.[21] In particular, vibrational spectroscopy appears useful for a distinction between mono- and bidentate nitrato ligands: both exhibit one mode near 1000 cm^{-1} and two bands at higher frequencies, where the splitting of the two latter is about 200 cm^{-1} for monodentate nitrato complexes and significantly larger in a bidentate situation. With the aim of providing a detailed molecular description, we report here on a joint experimental and theoretical study on micro-hydrated magnesium-nitrate cations $[MgNO_3(H_2O)_n]^+$ with up to 7 water ligands, including the gas-phase infrared spectrum of the mass-selected cation $[MgNO_3(H_2O)_3]^+$.

Results and discussion

Electrospray ionization of an aqueous solution of magnesium(II) nitrate leads to a series of coordination complexes $[MgNO_3(H_2O)_n]^+$ with a maximal value of $n = 7$ and the expected isotope patterns;[22] under mildest conditions of ionization, also signal corresponding to $n = 8$ and 9 are observed, but these were too weak for further characterization by means of tandem mass spectrometry. Upon sequentially change of the ionization process to more drastic conditions,[23,24] consecutive losses of water ligands are observed to finally afford the bare ionic core $[MgNO_3]^+$ upon complete desolvation.

CID spectra. Very similar to the behavior at increasingly harsher ionization conditions, the collision-induced dissociation (CID) spectra of mass-selected $[MgNO_3(H_2O)_n]^+$ ions (n = 1 - 7) display the evaporation of neutral water as the exclusive fragmentation channels throughout the range of collision energies studied (E_{lab} = 0 - 20 eV). In none of the CID spectra, a significant fragmentation of the nitrato-ligand in the $[MgNO_3(H_2O)_n]^+$ complexes is observed, whereas the bare ion $[MgNO_3]^+$ can be used as a precursor for the generation of the gaseous MgO^+ cation.[25] We note in passing that for n = 1, also the formation of small amounts of new complexes formed via endothermic ligand exchange with the collision gas xenon are observed, e.g. the cations $[Mg(Xe)]^+$ and $[MgNO_3(Xe)]^+$; the formation of similar rare-gas compounds has already been reported for gaseous magnesium(I) complexes.[26]

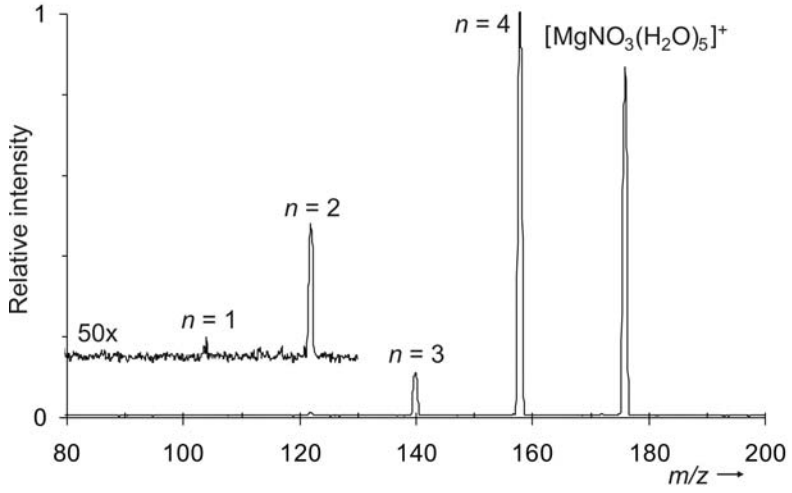

FIGURE 1. CID SPECTRUM OF MASS-SELECTED $[^{24}MgNO_3(H_2O)_5]^+$ (M/Z = 176) SHOWING THE CONSECUTIVE LOSSES OF WATER LIGANDS AT A COLLISION ENERGY OF 10 EV (LABORATORY FRAME) USING XENON AS A COLLISION GAS; THIS CORRESPONDS TO A COLLISION ENERGY OF E_{CM} = 4.3 EV IN THE CENTER-OF-MASS FRAME. THE LOW-MASS PART OF THE SPECTRUM INCLUDING THE SIGNALS FOR $[MgNO_3(H_2O)]^+$ (M/Z = 104) AND $[MgNO_3(H_2O)_2]^+$ (M/Z = 122) IS ALSO SHOWN WITH MAGNIFICATION BY A FACTOR OF 50.

As a representative example, the CID spectrum of $[MgNO_3(H_2O)_5]^+$ is shown in Figure 1. Clean sequential losses of up to four water ligands are observed without any evidence for the active

participation of the nitrato ligand. The abundances of the $[MgNO_3(H_2O)_{5-n}]^+$ fragment ions show a continuous decrease with increasing degree of fragmentation and are, of course, dependent on the actual collision energy adjusted in the experiments. In the example shown in Figure 1, the collision energy is fairly sufficient to induce multiple dehydrations down to the monosolvated ion $[MgNO_3(H_2O)]^+$.

As far as the CID spectra for varying numbers of water ligands are concerned, we refrain from a detailed presentation of all separate results and instead summarize the results for the mass-selected $[MgNO_3(H_2O)_n]^+$ ions (n = 1 - 7) at a collision energy of 1 eV (center-of-mass frame). The following trends can be observed in Figure 2. At first, the intensity of the parent ion decreases with n in that fragmentation is very weak for the monoligated magnesium-nitrate cation (n = 1), gradually increases for n = 2 and 3, whereas more than 50 % of the parent ions undergo fragmentation for n > 3, indicating that the further water molecules are much weakly bound (see section below). In the case of n = 5, the relative abundance of the loss of one water ligand does not increase any further, due to the competing evaporation of two neutral water molecules and to a small amount even more. The consecutive losses of solvent molecules reflect the decreasing binding energies and are of similar importance for the higher members with n = 6 and 7. Another notable effect is the increased relative abundance of the multiple water losses when going from n = 5 to n = 6. This observation may serve as a first indication for the existence of a structural difference between the complexes $[MgNO_3(H_2O)_5]^+$ and $[MgNO_3(H_2O)_6]^+$ sampled in the ESI experiments (see below).

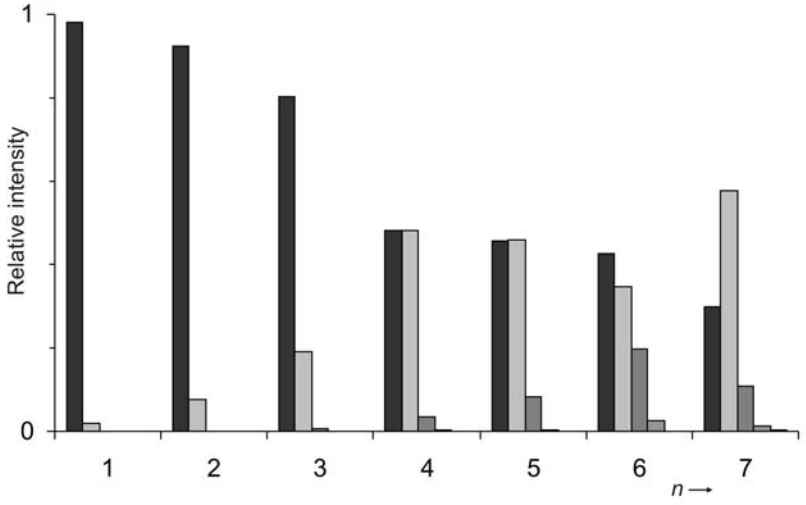

FIGURE 2. SUMMARIZED CID SPECTRA OF MASS-SELECTED $[MgNO_3(H_2O)_n]^+$ CATIONS AT AN AVERAGED COLLISION ENERGY OF 1.0 EV (CENTER-OF-MASS FRAME) AS A FUNCTION OF n. THE PARENT ION IS SHOWN AS A BLACK COLUMN, AND THE CONSECUTIVE WATER LOSSES ARE DISPLAYED AS GREY COLUMNS. DATA NORMALIZED TO Σ = 1. NOTE THAT THE PARENT IONS DO NOT DISAPPEAR COMPLETELY BECAUSE A SIGNIFICANT FRACTION OF THE INCIDENT IONS ENTERING THE HEXAPOLE REGION DO NOT UNDERGO ANY COLLISION AT ALL.

Further, the phenomenological appearance energies (*AEs*) derived from energy-dependent CID studies (see experimental details) are listed in Table 1. However, for the analysis of the thermochemistry of the $[MgNO_3(H_2O)_n]^+$ cations, we rather refer to the computed data, which can assumed to be reasonably reliable,[27,28] whereas the experimental data are obscured by the lack of ion thermalization in our experiments as well as the kinetic energy spread of the incident beam. The appearance energies given in Table 1 are thus just to be taken as a rough guidance. As expected for successive ion solvation, the *AEs* decrease with increasing *n*, and for the larger clusters with $n > 4$, a significant amount of dissociation is observed even at a nominal collision energy of 0 eV.

TABLE 1. AMOUNT OF DISSOCATION AT A COLLISION ENERGY NOMINALLY SET TO 0 EV (x_0 GIVEN AS THE FRACTION OF THE SUM OF ALL IONS) AND PHENOMENOLOGICAL APPEARANCE ENERGIES (*AEs* IN EV) FOR THE LOSS OF ONE WATER MOLECULE UPON CID OF MASS-SELECTED $[MgNO_3(H_2O)_n]^+$ IONS.[a]

n	1	2	3	4	5	6	7
x_0	0.005	0.03	0.07	0.16	0.20	0.23	0.55
AE	1.4	1.0	0.6	0.3	0.1	0.1	-0.05[b]

[a] For the determination of the *AEs*, see experimental details. [b] The negative value arises from the extrapolation procedure of the *AEs* at low binding energies and does not have a physical meaning.

Exchange experiments with D_2O. Complementary to CID, further insight into the ion structures can be gained by ion/molecule reactions. In this respect, reactions of the mass-selected $[MgNO_3(H_2O)_n]^+$ ions with an excess of D_2O appear as ideal probe, because the reaction with heavy water represents a minimal perturbation of the system, while allowing an investigation of the bound water ligands. Note in this context that we deliberately left the single-collision regime in order to also monitor consecutive exchange reactions. In general, three kinds of reactions take place. (i) For small numbers of *n*, notable amounts of association leading to $[MgNO_3(H_2O)_n(D_2O)]^+$ are observed ($n = 0$ - 3), where the abundance of this channel decreases with size, as expected from decreasing binding energies. (ii) For large numbers of *n*, an appreciable fraction of dissociation to the next smaller cluster $[MgNO_3(H_2O)_{n-1}]^+$ is observed even at a collision energy nominally set to 0 eV. Water loss is obviously an endothermic process, and the energy required for this process is either delivered by collisions of the neutral gas with fast ions present within the kinetic energy distribution of the mass-selected ion beam (*FWHM* = ca. 0.4 eV in the laboratory frame) or by the thermal energy content of the ions as well as the collision gas, because the binding energies are expected to reach thermal energies for large values of *n* (see below).[29] (iii) Last but not least, degenerate exchange takes place to afford the corresponding clusters $[MgNO_3(H_2O)_{n-1}(D_2O)]^+$ containing one D_2O ligand. Because the pressure of D_2O was adjusted to also allow for the occurrence of multiple collisions, all ions formed primarily according to (i) - (iii) can subsequently undergo exchange reactions. For a given $[MgNO_3(H_2O)_n]^+$ cluster, the ion/molecule reactions accordingly afford (i) the ligand-loss products $[MgNO_3(H_2O)_{n-m-1}(D_2O)_m]^+$ with *m* ranging from 0 to (*n*-1), (ii) the

association products $[MgNO_3(H_2O)_{n-m}(D_2O)_{m+1}]^+$ with m from 0 to n, and (iii) the exchange products $[MgNO_3(H_2O)_{n-m}(D_2O)_m]^+$ with m from 1 to n.

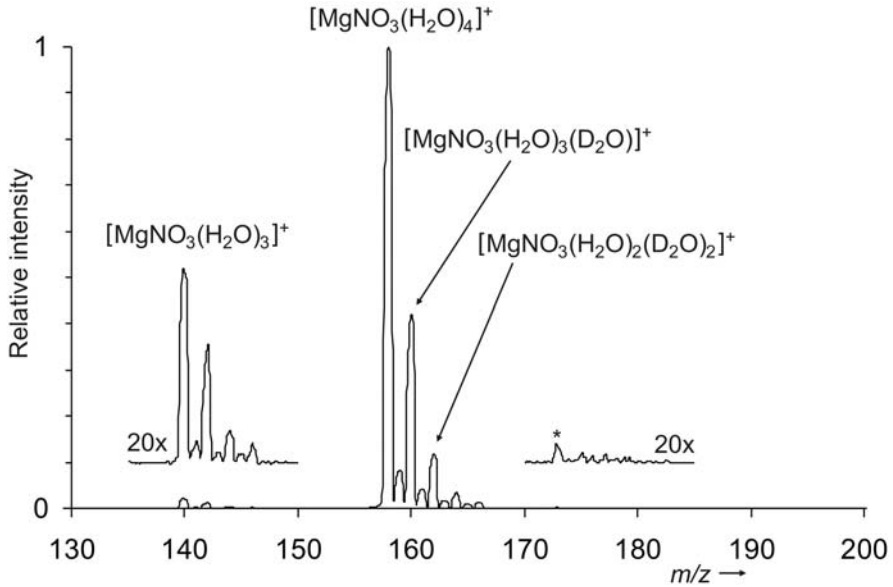

FIGURE 3. ION/MOLECULE REACTION OF MASS-SELECTED $[MgNO_3(H_2O)_4]^+$ CATIONS WITH D_2O AT A COLLISION ENERGY SET TO NOMINALLY 0 EV. RIGHT TO THE PARENT ION, CONSECUTIVE EXCHANGES OF H_2O BY D_2O LIGANDS ARE OBSERVED (SEE TEXT FOR HDO COMPLEXES). THE INSETS SHOW UNIMOLECULAR AND/OR COLLISION-INDUCED LOSS OF WATER LIGANDS CONCOMITANT WITH EXCHANGE (LEFT INSET) AND THE REGION FOR THE ADDITION OF WATER (RIGHT INSET), IN WHICH THE WEAK SIGNALS OBSERVED CAN BE ATTRIBUTED TO REACTIONS WITH CH_3OD BEING PRESENT AS A TRACE CONTAMINATION IN THE INLET SYSTEM; E.G., THE SIGNAL DENOTED WITH AN ASTERIX IS DUE TO $[MgNO_3(H_2O)_3(CH_3OD)]^+$.

For illustration, Figure 3 shows the reaction of mass-selected $[MgNO_3(H_2O)_4]^+$ with D_2O as an example. The major process occurring for this cluster size is the degenerate exchange of one H_2O ligand by D_2O, giving rise to peaks with a spacing of Δm = +2 at the right side of the parent-ion beam. Due to the consecutive nature of the ligand-exchange reactions, the abundances of the so-formed $[MgNO_3(H_2O)_{4-m}(D_2O)_m]^+$ ions decrease with m, but also complete exchange to $[MgNO_3(D_2O)_4]^+$ is visible in Figure 3 (Δm = +8).

In addition, also some ions with odd mass differences are observed (Δm = +1, +3, +5, and +7), which can, however, completely be traced back to residual HDO present in the reaction chamber. This is a crucial aspect in many isotope-exchange experiments with reagents having labile protons, because even though the supplied bulk reagents used may bear a high degree of isotope enrichment (here: D_2O, Aldrich, 99 atom-% D), protic adsorbates being present in the inlet system and the reaction chamber itself as well as water, which generally is a major component of the background gases in mass spectrometers in general and in the present experiments also originates from the aqueous solution used in the ESI source. Prior to any conclusion about the occurrence of partial H/D exchange reactions between the water ligands, it is therefore necessary to directly establish the actual degree of deuteration relevant in experiments. To this end, the association reaction of the

bare magnesium nitrate reaction $[MgNO_3]^+$ with the neutral water isotopologs present in the reaction cell was monitored, because it only gives rise to the product ions $[MgNO_3(H_2O)]^+$, $[MgNO_3(HDO)]^+$, and $[MgNO_3(D_2O)]^+$, whose relative abundances are a direct measure for the deuterium content. While the actual ratio is subject to some day-to-day variations, it was in the order of 85 atom-% D in the course of the measurements reported here. When the limited degree of deuteration is acknowledged in the quantitative evaluation of the data, all peaks at odd masses can be fully accounted for by the residual HDO present in the reaction chamber. In other words, inter-ligand H/D exchange reactions do not take place to a considerable extent for any of the $[MgNO_3(H_2O)_n]^+$ ions investigated. It is interesting to compare this finding with results of Sun *et al.* for ionic water clusters, who found that the proton-bound clusters $[H^+(H_2O)_n]$ easily undergo H/D exchange between the water ligands, whereas related open-shell cluster anions, such as $[H_2O^-{}^\bullet(H_2O)_n]$ and $[O_2^{-\bullet}(H_2O)_n]$, only exchange intact H_2O against D_2O units.[30]

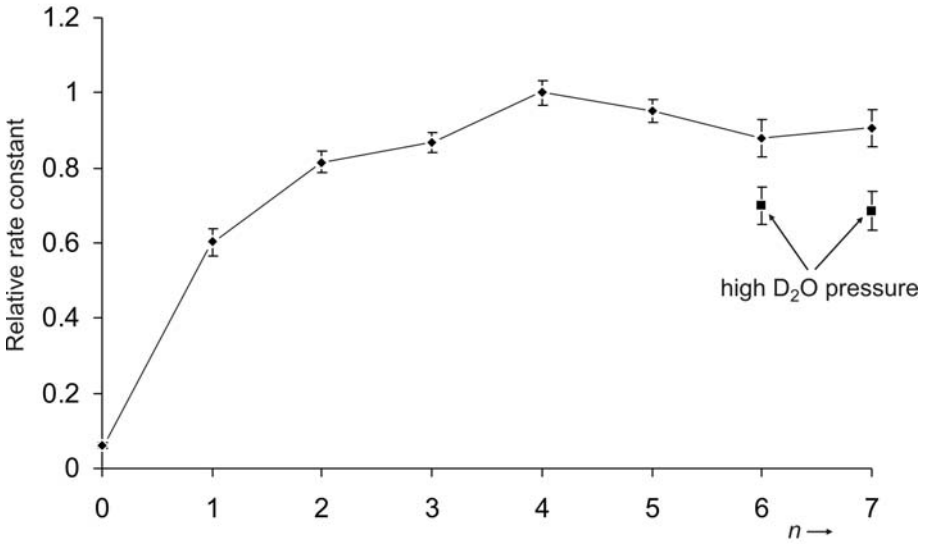

FIGURE 4. RELATIVE REACTION EFFICIENCY FOR DEGENERATE H_2O/D_2O EXCHANGE OF MASS-SELECTED $[MgNO_3(H_2O)_n]^+$ CATIONS WITH D_2O AS A FUNCTION n. NOTE THAT FOR $n = 0$, THE ENTRY CORRESPONDS TO THE ASSOCIATION OF BARE $[MgNO_3]^+$ WITH D_2O TO FORM $[MgNO_3(D_2O)]^+$. UNLESS NOTED OTHERWISE, THE DATA REPRESENTED BY RHOMBIC SYMBOLS (♦) ARE AVERAGES OF THREE INDEPENDENT MEASUREMENTS AT DIFFERENT PRESSURES RANGING FROM $p(D_2O) = 0.8 - 4 \cdot 10^{-4}$ MBAR. FOR $n = 6$ AND 7, HOWEVER, THE DATA AT HIGH PRESSURES (■) DEVIATE SIGNIFICANTLY; SEE TEXT.

Figure 4 shows the experimentally measured relative reaction efficiencies of the D_2O exchange for the $[MgNO_3(H_2O)_n]^+$ clusters with n = 0 - 7; for n = 0, the entry corresponds to the mere addition of D_2O, otherwise, only the exchange channel is included in the analysis. These experiments were performed at different pressures of neutral D_2O in order to deliberately allow for multiple collisions and thus consecutive exchanges of the water ligands. Data analysis with regard to relative rate constants accordingly refers to the sum of all exchange products relative to the parent ion at a given pressure of D_2O. Inspection of the data shown in Figure 4 reveals reaction

efficiencies increasing with *n*, which is to be expected for statistical reasons. In the case of $[MgNO_3(H_2O)]^+$, for example, the maximum rate constant to be expected amounts to half of the gas-kinetic collision rate, because the intermediate encounter complex $[MgNO_3(H_2O)(D_2O)]^+$ being formed can lose either light of heavy water in a 1 : 1 ratio if isotope effects are neglected (see below). For $[MgNO_3(H_2O)_2]^+$, already 2/3 of the collision rate can be expected on the same grounds. The relative rates are accordingly anticipated to scale with approximately $n/(n+1)$, resulting in an approach to unit collision rate for large values of *n*.

Overall, the experimental data shown in Figure 4 confirm the expected statistical behavior, even though the larger clusters show a slightly lower rate of exchange. However, for the largest clusters $[MgNO_3(H_2O)_6]^+$ and $[MgNO_3(H_2O)_7]^+$ the relative rates obtained at higher pressures of water are significantly lower compared to those obtained at lower D_2O pressure. As one possible explanation for this observation we propose that the larger clusters are formed as a mixture of structural isomers, of which the one undergoes the exchange reaction more rapidly than the other. Due to the fact that in the multipole set-up used in these experiments, the pressure of the neutral reactant rather than time is used as variable in kinetic measurements, the presence of a less reactive isomer will accordingly lead to a lowered relative conversion at increased pressure and thus lowered apparent rate constants. We also note that the anticipated isomeric clusters might also result from a cooling effect under multiple collision conditions, in that the temperature of the clusters might be lowered that much that the water molecules in the inner solvation shell do less efficiently participate in the exchange process.

While this issue could be addressed by a careful analysis of the exchange kinetics, we refrain from such an effort in the present experiments, because the multipole set-up used is not ideally suited to probe consecutive ion/molecule reactions. This is primarily due to the non-negligible kinetic energy distribution of the incident beam which prevents the description of consecutive reactions by a single set of rate constants.[31] Specifically, we found that the apparent rates of the consecutive exchange reactions increase with the number of incorporated D_2O molecules. In the case of $[MgNO_3(H_2O)_4]^+$, for example (see Figure 3), the relative rate constants for the exchange of the first to forth H_2O ligands as determined by kinetic modeling[31-33] scale as 1.00 : 1.13 : 1.28 : 1.44, whereas from pure statistics one would in fact expect a decrease of the propensity for H_2O/D_2O exchange according to 4/5 : 3/5 : 2/5 : 1/5. This effect can be understood by reference to the kinetic-energy spread of the incident beam. Because this aspect is of more general relevance for the analysis of consecutive reactions in beam-type mass spectrometers, we briefly address it in some more detail. Thermal ion/molecule reactions, degenerate isotope exchange in particular, generally show a pronounced negative temperature/energy behavior because the degree of equilibration within the collision complex is decisively determined by its lifetime, which in turn

crucially depends on the energy of the collision complex. The larger the energy is, the shorter the intermediate's lifetime is, and consequently less exchange can take place. In the experiments described above, mass-selected ion beams with a kinetic energy distribution having a half-width of about 0.4 eV are sampled. Of these ions, the faster moving fraction will undergo exchange with a lower rate than the slow ions; the actual measurement will average over all contributions, however. For an illustration of the consequences of this situation, let us refer to a "hypothetical experiment" (Figure 5).

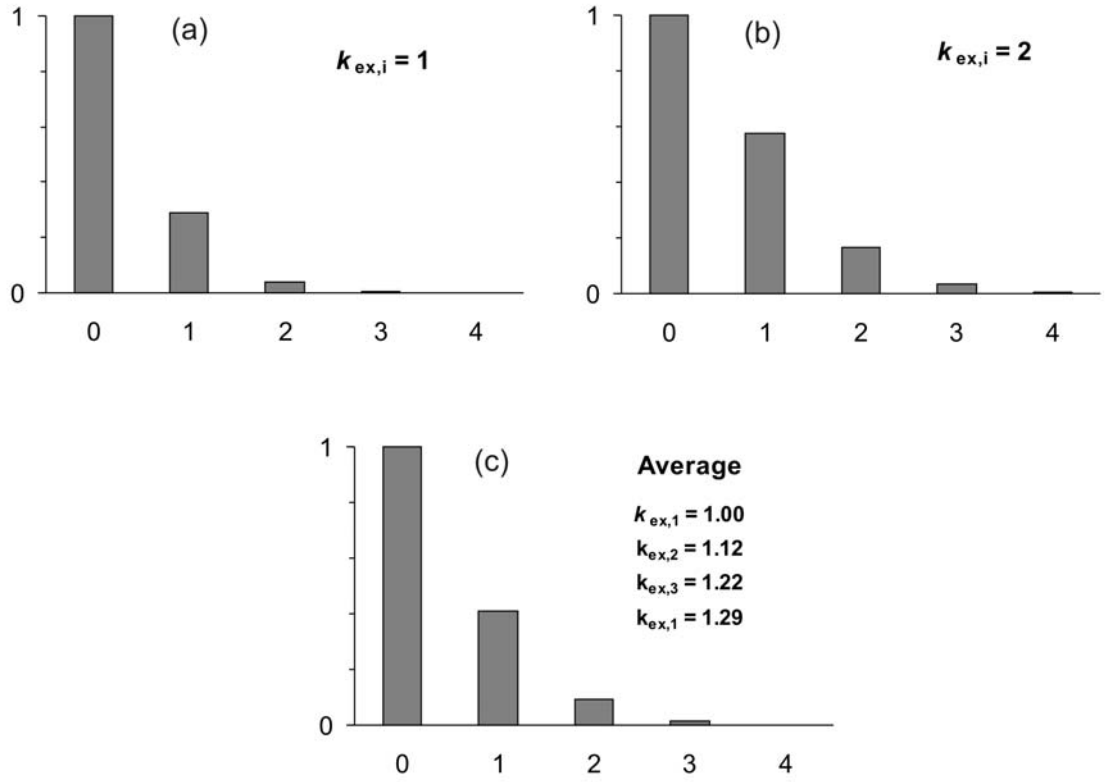

FIGURE 5. HYPOTHETICAL PRODUCT PATTERN FOR THE DEGENERATE H_2O/D_2O EXCHANGE OF $[MgNO_3(H_2O)_4]^+$ WITH D_2O FOR (A) EQUAL RATE CONSTANTS $k_{ex,i}$ = 1 (i = 1 - 4) AND (B) EQUAL RATE CONSTANTS $k_{ex,i}$ = 2 (i = 1 - 4) AND (C) THE AVERAGE OF THE PRODUCT DISTRIBUTIONS IN FIGURES 5A AND 5B. NOTE THAT THE RESULTING APPARENT RATE CONSTANTS LISTED IN FIGURE 5C INCREASE WITH THE PROGRESSION OF LIGAND EXCHANGE; SEE TEXT.

Figure 5a shows the exchange pattern simulated for $[MgNO_3(H_2O)_4]^+$ at 25 % conversion of the parent ion, where, for the sake of simplicity, we assume equal rate constants of $k_{ex,i}$ = 1 for all four exchanges possible. While Figure 5a shall represent a fraction of the ion beam with relatively high kinetic energy, the slower ions will undergo exchange more rapidly; $k_{ex,i}$ = 2 is assumed in the hypothetical case of Figure 5b. The ion-beam experiments themselves represent the integral kinetic energy distribution, which is simplified in Figure 5c as the arithmetic average of the distributions in Figures 5a and 5b. When the resulting pattern in Figure 5c is analyzed in terms of a kinetic

modeling,[31-33] the apparent rate constants show an increase with increasing progression of isotope exchange as indicated in the Figure. The algebraic reason for this kinetically not meaningful order of rate constants is that the attempt to model the energy distributions sampled in the experiments with a single set of rate constants requires larger rate constants for the consecutive steps in order to cope for the increased amount of multiple exchange for the slow moving ions (see Figures 5a versus 5b). We note further that the increase of the relative rate by only a factor of 2 is a conservative estimate because thermal ion-molecule reactions often show rather steep negative energy dependence.

While it would be possible to deconvolute the energy distributions by careful analysis of the kinetic energy behavior, such an attempt is per se associated with considerable error margins. In general, we therefore conclude that ion-trap based studies are much more suitable for a detailed kinetic analysis of consecutive reactions, being it ligand exchange of hydrated metal ions[29,30,34-36] or even complex catalytic cycles of gaseous ions.[37-39] These arguments notwithstanding, the rate constants of the initial exchange in the ion-beam experiments described above can yet be assumed as a representative measure for the cluster-ion structures.

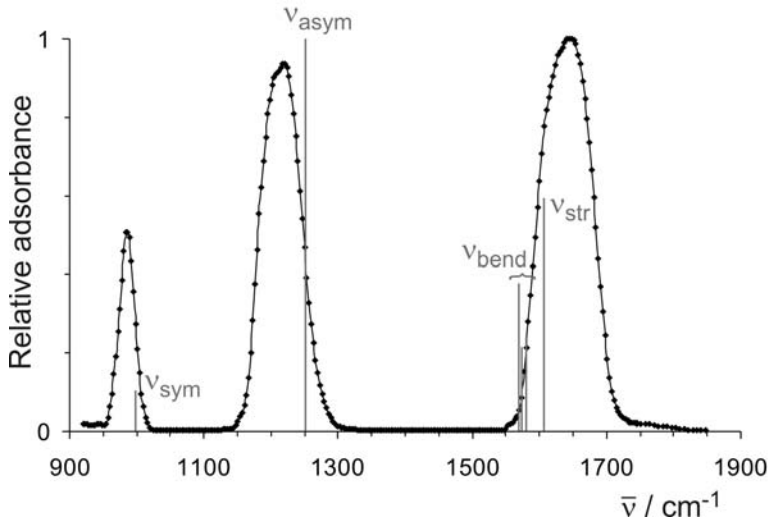

FIGURE 6. EXPERIMENTAL IRMPD SPECTRUM OF MASS-SELECTED $[Mg(NO_3)(H_2O)_3]^+$ (DATA POINTS ARE THE AVERAGE OF TWO INDEPENDENT SPECTRA AND ARE GIVEN AS ♦) AND COMPUTED IR MODES IN THIS SPECTRAL RANGE (GREY BARS).

IRMPD experiments. Recently, infrared multiphoton-induced photodissociation (IRMPD) of mass-selected ions has been introduced as a powerful tool for the elucidation of the structures of gaseous ions.[40] In the anticipation of achieving experimental evidence for the formation of solvent-separated ion pairs, some gas-phase IRMPD spectra of mass-selected $[MgNO_3(H_2O)_n]^+$ ions were accordingly recorded using an ion-trap mass spectrometer (ITMS) equipped with an ESI source, which is mounted at the infrared-laser facility CLIO.[41,42] Figure 6 shows the IRMPD spectrum of $[MgNO_3(H_2O)_3]^+$ between 900 and 1900 cm^{-1}, which corresponds to the spectral range investigated

at CLIO. In the experiment, three bands at ca. 985 cm^{-1}, 1215 cm^{-1}, and 1640 cm^{-1} are observed. According to the literature,[21] the large spacing of the two latter bands suggests a bidendate coordination, as also predicted by theory (see below). Further, comparison of the computed frequencies (scaled with 0.96 as recommended by Scott and Radom)[43] shows reasonable, although by no means perfect agreement with experiment. Specifically, the computations predict six IR active modes for the $[MgNO_3(H_2O)_3]^+$ ion in the wavelength range probed by IRMPD: a symmetrical ($\nu_{sym}(NO_3)$: 998 cm^{-1}, 54 km mol^{-1}) and asymmetrical ($\nu_{asym}(NO_3)$: 1252 cm^{-1}, 533 km mol^{-1}) stretch of the nitrato ligand, three, almost degenerate bending modes of the coordinated water molecules ($\nu_{bend}(H_2O)$: 1573 cm^{-1}, 200 km mol^{-1}; 1575 cm^{-1}, 114 km mol^{-1}; 1582 cm^{-1}, 127 km mol^{-1}), and the stretching mode of the NO unit ($\nu_{str}(NO)$: 1609 cm^{-1}, 316 km mol^{-1}).

Interestingly, the formal widths at half height of the three peaks observed experimentally appear to increase with increasing wavenumber, i.e. $b_{1/2}$ = 20 cm^{-1} for the peak centered at 985 cm^{-1}, $b_{1/2}$ = 60 cm^{-1} for the band at 1215 cm^{-1}, and even $b_{1/2}$ = 90 cm^{-1} for the adsorption at about 1640 cm^{-1}. For the latter band, this effect can be understood because four different modes contribute to it and uncertainties in the predicted frequencies in conjunction with the expected line-width in the order of about 20 cm^{-1} in the experimental set-up used[41] may well give rise to a broadened peak. The remarkable difference between the bands at 985 cm^{-1} and 1215 cm^{-1} of the nitrato ligand does not find a rationale, however. Considering the large infrared cross-section calculated for the asymmetric NO stretch, saturation might occur for the band at 1215 cm^{-1}. Further, recent spectroscopic observations for related solvated sulfate dianions $[SO_4 (H_2O)_n]^{2-}$ also show line broadenings, which are associated with excited torsional or librational states with short lifetimes.[44,45] Thus, it appears quite conceivable that the couplings of symmetric and asymmetric NO stretches with the vibrational bath are so different that they experience different broadening effects.

Unfortunately, however, it turned out that in the ITMS set-up used here only this particular complex could be investigated with IRMPD. For the other $[MgNO_3(H_2O)_n]^+$ ions, the experimental conditions in the ITMS were not suitable. Specifically, the ions with lower coordination (n = 1, 2) undergo association reactions with water present in the background vacuum of the ITMS to afford ions with larger n during the time interval required for triggering with the laser and the interaction with the laser pulses (ca. 1 second). In the case of n = 1, for example, in the absence of IR irradiation more than 70 % of the incident ions undergo association to $[MgNO_3(H_2O)_2]^+$ during storage in the ion trap. In the opposite, the solvated magnesium-nitrate cations with larger values of n are not stable under the conditions of ITMS due to their low binding energies, such that the rf-energy continuously admitted to the ions stored in the trap in conjunction with the helium serving as a collision gas leads to CID of these more weakly bound clusters. In order to test the latter

hypothesis and to exclude that the solvated $[MgNO_3(H_2O)_n]^+$ ions with $n > 3$ are intrinsically short-lived, these were also investigated in a ion-cyclotron resonance mass spectrometer, in which these species can be stored within the second timescale without any considerable ion losses. We are accordingly left to conclude that the set-up of the ITMS is of inherently limited suitability for the investigation of weakly bounded solvent clusters.

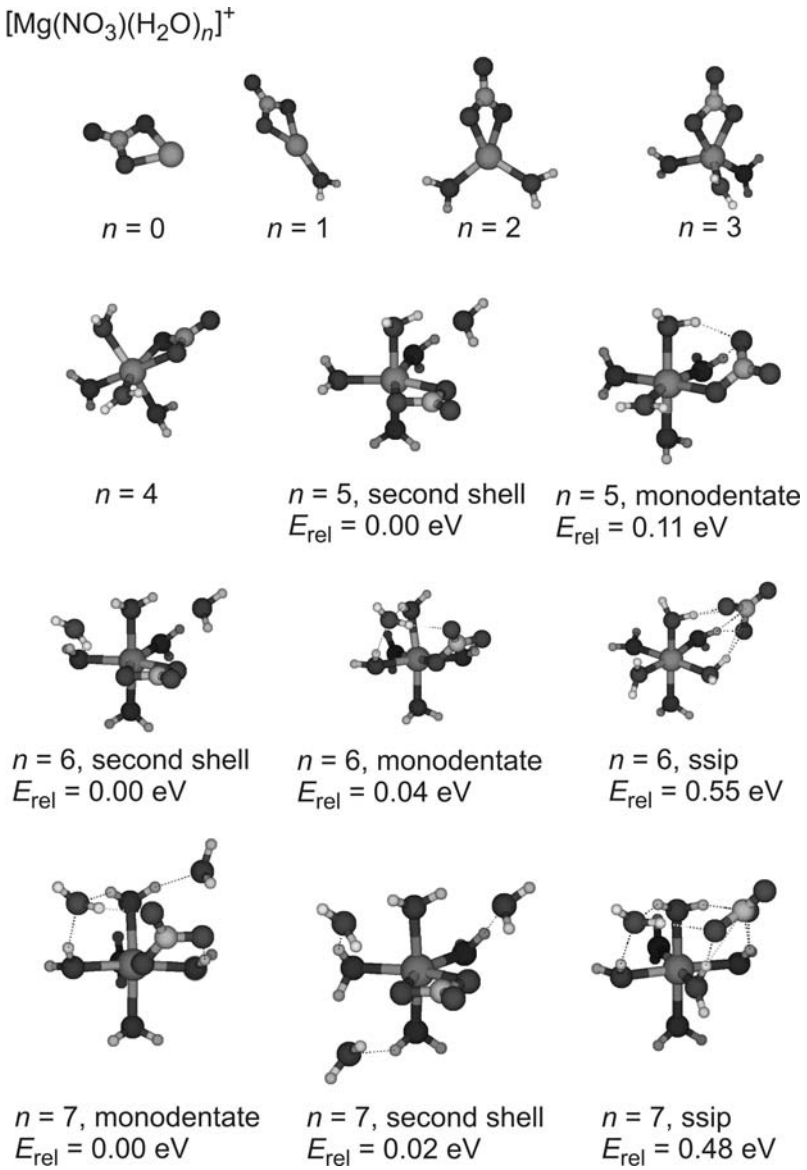

FIGURE 7. OPTIMIZED GEOMETRIES OF $[MgNO_3(H_2O)_n]^+$ CATIONS AT THE MP2/DZP LEVEL OF THEORY. THE THIN DOTTED LINES INDICATE THE NETWORK OF HYDROGEN BONDS ESTABLISHED IN THE CLUSTERS WITH LARGER VALUES OF *n*. THE ABBREVIATION SSIP STANDS FOR STRUCTURES WHICH CAN BE TERMED AS SOLVENT-SEPARATED ION PAIRS OF THE TYPE $[Mg(H_2O)_n^{2+}]\bullet[NO_3^-]$.

Theoretical results. For a computational survey of the $[MgNO_3(H_2O)_n]^+$ ions (n = 0 - 7), we have chosen the MP2/aug-cc-pVDZ approach with a medium-sized basis set as a reasonable compromise between reliability and computational costs.[27,28] We further note that the structures of bare $[MgNO_3]^+$ as well as the monohydrate $[MgNO_3(H_2O)]^+$ were previously investigated using HF

methods,[19] and that the hexacoordinated magnesium clusters with n = 4 and 5 have already been studied by Zhang et al., who performed RHF/6-311++G calculations.[16]

According to our computational results, successive addition of water ligands to the C_{2v}-symmetric $[MgNO_3]^+$ core ion (n = 0, Figure 7) first occurs from the opposite side of the bidentate nitrato ligand with trigonal, quasi-tetrahedral, and quasi-trigonalpyramidal arrangements, respectively (see structures for n = 1 - 3 in Figure 7). Incorporation of a fourth water ligand to $[MgNO_3(H_2O)_3]^+$ requires some structural reorganization leading to a quasi-octahedral structure in which magnesium has reached the coordination number 6 (n = 4, Figure 7). Consequently, a fifth water ligand can either begin to form a second solvation shell, that is hydrogen bonding with the existing water ligand, rather than direct coordination to magnesium, or induce a change of the local coordination geometry of the nitrato ligand from bi- to monodentate, thereby providing another vacancy in the quasi-octahedral coordination sphere (see the two structures for n = 5 in Figure 7). Of these two options, the one with one water molecule in the second shell is energetically preferred by 0.11 eV over the monodentate alternative. Interestingly, this lowest-lying geometry was not identified in the previous computational study,[14] which reported only the energetically more demanding monodentate structure. In addition to these two types of structures, even another option comes into play for the presence of six water ligands in that all water molecules may form a perfect octahedral environment around the magnesium, which hence exists as a dication with a nitrate counterion in close vicinity and additionally stabilizing hydrogen bonds (see the three structures for n = 6 in Figure 7). However, although the structure of the solvent-separated ion-pair is a well-defined local minimum for n = 6, it is still 0.55 eV above the most stable structure with two water molecules in the second shell and also 0.51 above the isomer with monodentate nitrate. Finally, in the case of n = 7 the monodentate structure is computed as to be even slightly more stable (0.02 eV) than that with three water molecules in the second solvation shell, most likely due to the preferable network of hydrogen bonds in the case of the former (see structures for n = 7 in Figure 7). Also for n = 7 the solvent-separated ion-pair has been located as a local minimum, which is still about 0.48 eV higher in energy than the conventional coordination structures.

TABLE 2. COMPUTED TOTAL ENERGIES (IN HARTREE), ADIABATIC WATER BINDING ENERGIES ($\Delta_r H$ AT 0 K IN EV) FOR THE LOSS OF ONE WATER MOLECULE AND THE CORRESPONDING FREE ENERGIES ($\Delta_r G$ AT 298 K IN EV) FOR HYDRATED $[MgNO_3(H_2O)_n]^+$ IONS WITH $n = 0$ - 7.[a,b]

n	E_{tot}	$\Delta_r H$ (0 K)	$\Delta_r G$ (298 K)
0[c]	- 479.11627		
1	- 555.45776	2.10	1.77
2	- 631.78169	1.61	1.23
3	- 708.09239	1.27	0.88
4	- 784.39068	0.90	0.46
5[c]	- 860.68156	0.69	0.28
6[d]	- 936.97228	0.68	0.25
7[e]	- 1013.26075	0.62	0.21
H_2O[f]	- 76.26091		

[a] Only the most stable isomers are listed. [b] 1 Hartree = 27.2115 eV. [c] Entry corresponds to the isomer with one water molecule in the second solvation shell (see Figure 7, $n = 5$). The structure with monodentate nitrate is 0.11 eV higher in energy. [d] Entry corresponds to the isomer with two water molecule in the second solvation shell (see Figure 7, $n = 6$). The structure with monodentate nitrate is only 0.04 eV and the ion-pair structure 0.55 eV higher in energy. [e] Entry corresponds to the isomer with monodentate nitrate (see Figure 7, $n = 7$). The structure with three water molecules in the second solvation shell is only 0.02 eV and the ion-pair 0.48 eV higher in energy. [f] The total energies of bare $[MgNO_3]^+$ and water are given for the sake of completeness; the computed zero-point energies of $[MgNO_3]^+$ and H_2O are 0.01649 and 0.02133 Hartree, respectively.

With respect to the mass spectrometric experiments, the key parameters are the sequential water binding energies of the hydrated magnesium-nitrate cation, which are summarized in Table 2. As expected, the magnitude of $\Delta_r H$ decreases from a 0 K value of 2.1 eV for the monohydrated ion to about 0.7 eV for the largest values of n examined in this work. Even more pronounced is the decrease in the free energies $\Delta_r G$, which fall from 1.77 eV to only about 0.25 eV for $n = 5$ - 7. Further, the finding that the binding energies appear to reach a plateau at about for $n = 5$ - 7 is perfectly consistent with the anticipated bonding situations (see Figure 7) in that the bonds of the new incoming water ligands are not anymore formed to the electropositive metal core, but involve hydrogen bonds to the coordinated water molecules. It is interesting to note that these energies converge close to the bulk value of 0.21 eV per hydrogen bond in water, rather than to the bulk water binding energy which is somewhat higher.[46] This observation is consistent with the view that the outer, mostly weakly bound water molecules in the $[MgNO_3(H_2O)_n]^+$ ions are only partially coordinated compared to the network of hydrogen bonds existing in bulk water.

In the context of the ion/molecule reactions with heavy water, we also computed the equilibrium isotope effects associated with the successive exchange of H_2O ligands in $[MgNO_3(H_2O)_6]^+$ by heavy water. The data given in Table 3 clearly indicate the operation of significant equilibrium isotope effects (EIEs), which favor the incorporation of heavy water in the cluster ion.[47] In exchange-experiments with heavy water, the EIE is accordingly expected to lead to an enrichment of the heavy water bound to the metal cation.[48,49] Moreover, there even exists a significant EIE as far as the position of the D_2O in the cluster is concerned. Thus, for the cluster with one heavy water, $[MgNO_3(H_2O)_5(D_2O)]^+$, we considered substitution of an internal and an outer water ligand by

heavy water. As shown in Table 3, direct coordination of D_2O at the magnesium is preferred over incorporation in the outer sphere (entries 2 and 3 in Table 3). Even though the effect is small (the *EIEs* differ by only 0.07), the results still suggest some enrichment of heavy water in the center of the water clusters.

TABLE 3. COMPUTED ENERGY DIFFERENCES (IN KJ MOL^{-1}) OF HEXAHYDRATED $[MgNO_3(H_2O)_{6-n}(D_2O)_n]^+$ IONS AS A FUNCTION OF D_2O CONTENT AND THE EQUILIBRIUM ISOTOPE EFFECTS (*EIES*) AT 298 K DERIVED THEREFROM. FOR THE CLUSTER WITH A SINGLE D_2O INCORPORATED, VALUES FOR TWO ISOMERS (D_2O INSIDE AND D_2O OUTSIDE) ARE GIVEN.

n	$\Delta\Delta_rH$ (0 K)	$\Delta\Delta_rH$ (298 K)	$\Delta\Delta_rG$ (298 K)	*EIE* (298 K)
0[a]	0.00	0.00	0.00	1.00
1_in[b]	-0.55	-0.32	-0.13	1.24
1_out[c]	-0.46	-0.23	-0.09	1.17
2	-1.06	-0.60	-0.23	1.48
3	-1.58	-0.91	-0.34	1.77
4	-1.98	-1.10	-0.42	2.04
5	-2.45	-1.33	-0.52	2.41
6	-2.92	-1.58	-0.62	2.83

[a] This row stands for $[MgNO_3(H_2O)_6]^+ + 6\ D_2O$ and serves the reference for the calculation of the energy differences and the *EIEs*. [b] Here, one of the inner water ligands opposite to the nitrate ion (see "second-shell" structure for $n = 6$ in Figure 6) is replaced by D_2O. [b] Here, one of the outer water ligands in top position (see "second-shell" structure for $n = 6$ in Figure 6) is replaced by D_2O.

Finally, let us discuss the implications of the theoretical results with regard to the exchange kinetics in the experiments with D_2O, which revealed indications for the presence of isomeric $[MgNO_3(H_2O)_n]^+$ clusters for $n = 6$ and 7. In this respect, the rather small energy differences computed between the monodentate structures and those in which the water only occupies the second solvation shell may serve as an explanation, but given the close structural similarities between these structures, their mutual interconversion can expected to be facile. Instead, presence of the solvent-separated ion pairs might explain the experimentally observed effects, because in these the water ligands are closely bound to the metal such that an incoming D_2O molecule might not easily promote exchange. Against this reasoning is the fact that these structures are computed to lie considerably higher in energy. Nevertheless, consideration of the process of electrospray ionization, a technique which samples the ions directly from solution, at least suggests that the solvent-separated ion pairs may be formed. Thus, in a diluted aqueous solution of $Mg(NO_3)_2$ almost complete heterolysis to $[Mg(H_2O)_n]^{2+}$ and $[NO_3(H_2O)_n]^-$ can in fact safely be assumed. In the ESI process, a $[Mg(H_2O)_n]^{2+}$ dication stemming from solution may hence loosely associate with a solvated counterion. Further evaporation of the solvent in the droplet then provides a straightforward access to the solvent-separated ion pairs, although these are not the most stable structures for $[MgNO_3(H_2O)_n]^+$ clusters with $n = 6$ and 7.

Conclusions

The micro-hydration of the $[MgNO_3]^+$ cation is studied in a joint experimental and theoretical study. The trends observed for the $[MgNO_3(H_2O)_n]^+$ clusters with n = 1 - 7 can be summarized as follows. (i) With increasing number of water ligands, the binding energies decrease and approach the strengths of hydrogen bonds in water due to the formation of a second solvation shell. (ii) Likewise, the tendency for monodentate coordination of the nitrato ligand increases with increasing hydration of the magnesium ion. (iii) Solvent-separated ion pairs with a genuine $[Mg(H_2O)_n]^{2+}$ dication and a (solvated) counterion in close proximity are, however, not energetically accessible at thermal energies. The results obtained in the exchange reactions with D_2O indicate, however, that for n = 6 and 7 formation of the solvent-separated structures might be kinetically favored in the ESI process. In a more general sense, the exchange experiments with D_2O offer an alternative method to probe micro-hydrated metal ions, which we will pursue in further studies of solvated metal ions. Moreover, it remains to be settled experimentally, whether clear evidence for the transition from the contact ion pairs with the anionic ligands directly bound to the metal cation and solvent separated ion pairs can be achieved in the future.

Experimental and theoretical methods

The experiments were performed using a VG BIO-Q mass spectrometer as described in detail elsewhere.[50] Briefly, the instrument consists of an electrospray ionization source combined with a tandem mass spectrometer of QHQ configuration (Q stands for quadrupole and H for hexapole). In the present experiments, mmolar solutions of magnesium(II) nitrate in pure water were introduced through a fused-silica capillary to the ESI source via a syringe pump (ca. 5 µl/min). Nitrogen was used as nebulizing and drying gas at a source temperature of ca. 120 °C. Maximal yields of the desired ions $[MgNO_3(H_2O)_n]^+$ (n = 1 - 7) were achieved by adjusting the decisive cone voltage to about 2 and 40 V, respectively.[23,24] For collision-induced dissociation (CID), the ions of interest were mass-selected using Q1, interacted with xenon as a collision gas in the hexapole H under single-collision conditions (typically $2 \cdot 10^{-4}$ mbar) at variable collision energies (E_{lab} = 0 - 20 eV), while scanning Q2 to monitor the ionic products.

As pointed out previously, the VG Bio-Q does not allow to directly extract quantitative threshold information from CID experiments due to several limitations of the commercial instrument.[50] For weakly bound ions,[51] for example, even at E_{lab} = 0 eV a non-negligible amount of ion decay is observed, which is in part attributed to the presence of collision gas not only in the hexapole, but also in the focusing regions between the mass analyzers. Note that these dissociations do not correspond to metastable ions because they do not occur in the absence of collision gas. To a first approximation, however, the energy dependence of the product distributions in the CID spectra can

be approximated by a sigmoid function,[52] which allows to extract some semi-quantitative information about the energetics of the ions examined.[53] The energy dependence of the CID fragments can hence be approximated by functions of the type $I_i(E_{CM}) = (BR_i/(1+e^{(E_{1/2}-E_{CM})b})$ using a least-square criterion; for the parent ion M, the relation is: $I_M(E_{CM}) = [1 - \Sigma(BR_i/(1+e^{(E_{1/2,i}- E_{CM})b_i})]$. Here, BR_i stands for the branching ratio of a particular product ion ($\Sigma BR_i = 1$), $E_{1/2}$ is the energy at which the sigmoid function has reached half of its maximum, E_{CM} is the collision energy in the center-of-mass frame ($E_{CM} = m_T/(m_T+m_I) \bullet E_{lab}$, where m_T and m_I stand for the masses of the collision gas and the ion, respectively), and *b* describes the rise of the sigmoid curve. In consecutive dissociations, all higher-order product ions were added to the intensity of the primary fragment. Further, non-negligible ion decay at $E_{lab} = 0$ eV as well as some fraction of non-fragmenting parent ions at large collision energies were acknowledged by means of appropriate scaling and normalization procedures. This empirical, yet physically reasonable approach is able to reproduce the measured ion yields quite well. It is obvious, however, that the term $E_{1/2}$ used in the exponent does not correspond to the intrinsic appearance energies of the fragmentation of interest, not to speak of the corresponding thermochemical thresholds at 0 K. The phenomenological threshold energies given below were derived from linear extrapolations of the rise of the sigmoid curves at $E_{1/2}$ to the base line.

For the reactivity studies with D_2O, the ions were mass-selected with Q1 at a mass-resolution sufficient to separate other than isobaric ions and then injected into the hexapole serving as a reaction chamber at a collision energy set to nominally 0 eV. By means of retarding-potential analysis, the kinetic-energy width of the primary ion beam was determined as 0.4 ± 0.1 eV (formal width at half maximum). We have demonstrated previously that under these conditions the VG BioQ can be used for the investigation of thermal ion/molecule reactions,[54-56] and that the initial rate constant show a linear dependence on the pressure of the neutral reagent;[25] except for the specific cases of $[MgNO_3(H_2O)_6]^+$ and $[MgNO_3(H_2O)_7]^+$, as discussed above. Further, in these ion/molecule reactions the pressure of the neutral reagent D_2O was deliberately extended beyond the regime of single-collision conditions in order to allow the occurrence of multiple exchange reactions,[55] which permits the investigation of the coordination sphere of the $[MgNO_3(H_2O)_n]^+$ complexes in more detail.

In addition, gas-phase infrared spectra of mass-selected $[MgNO_3(H_2O)_n]^+$ ions were recorded with an Bruker Esquire 3000 ion-trap mass spectrometer (IT-MS)[41,57,58] mounted to the beam line of a free electron laser at CLIO (Centre Laser Infrarouge Orsay, France). Briefly, the $[MgNO_3(H_2O)_n]^+$ ions of interest were generated by ESI of aqueous magnesium(II) nitrate and mass-selected in the ion trap. After mass selection, infrared multi-photon dissociation was induced by admittance of four

pulses of IR-laser light to the ion trap, resulting in a total trapping time of about one second. In the 40 - 45 MeV range in which CLIO was operated in these experiments, the IR light covers a range from about 900 to 1900 cm^{-1}. Effects of laser-power dependence and irradiation time were checked for in appropriate control experiments, and no other than the expected dependences were found.[59,60]

The calculations were performed with second order Møller-Plesset perturbation theory (MP2) utilizing the Gaussian 03 program package.[61] For all atoms, Dunning's augmented, correlation consistent, polarized double-zeta basis sets were used.[62] The nature of all stationary points as genuine local minima or saddle points was probed by analysis of the Hessian matrix. Energies are corrected for zero-point vibrational energy contributions and are reported as relative energies at 0 K as well as relative free enthalpies at 298 K, respectively. For each cluster size, geometry optimizations were started from various initial structures guessed by chemical intuition. For small clusters with several water molecules, this procedure provides all low-lying minima of the complexes after minimization. For larger clusters, we aimed at obtaining representative and (probably) lowest-lying structures. For even larger clusters, one should first perform a pre-search of the potential-energy surface using an annealing/quenching approach employing classical molecular dynamics; however, we did not attempt to apply this procedure for the small and medium-sized clusters investigated in this work.

Acknowledgement

D.S. thanks M. K. Beyer for a preprint of ref. 4 and is grateful to H. Schwarz (TU Berlin, Germany) for the opportunity to utilize the VG BioQ mass spectrometer for part of these measurements. P.M. and D.S. were supported by a travel grant of the European Commission to the European multi-user facility CLIO. P.J. acknowledges support from the Czech ministry of education (grant LC 512) and the Grant Agency of the Czech Republic (203/07/1006).

References

[1] P. Jungwirth, *J. Phys. Chem. A* **2000**, *104*, 145-148.
[2] X.-B. Wang, H.-K. Woo, B. Jagoda-Cwiklik, P. Jungwirth, L.-S. Wang, *Phys. Chem. Chem. Phys.* **2006**, *8*, 4294-4296.
[3] G. D. Markham, J. P. Glusker, C. W. Bock, *J. Phys. Chem. B* **2002**, *106*, 5118-5134.
[4] M. K. Beyer, *Mass Spectrom. Rev.*, in press.
[5] S. Petrie, *J. Phys. Chem. A* **2002**, *106*, 7034-7041.
[6] M. Peschke, A. T. Blades, P. Kebarle, *J. Phys. Chem. A* **1998**, *102*, 9978-9985.
[7] M. Beyer, E. R. Williams, V. E. Bondybey, *J. Am. Chem. Soc.* **1999**, *121*, 1565-1573.
[8] S. E. Rodriguez-Cruz, R. A. Jockusch, E. R. Williams, *J. Am. Chem. Soc.* **1999**, *121*, 1986-1987.
[9] S. E. Rodriguez-Cruz, R. A. Jockusch, E. R. Williams, *J. Am. Chem. Soc.* **1999**, *121*, 8898-8906.
[10] M. Peschke, A. T. Blades, P. Kebarle, *Int. J. Mass Spectrom.* **1999**, *187*, 685.
[11] S. E. Rodriguez-Cruz, R. A. Jockusch, E. R. Williams, *J. Am. Chem. Soc.* **1999**, *121*, 8898.

[12] N. Walker, N. P. Dobson, R. R. Wright, P. E. Barran, J. N. Murrell, A. J. Stace, *J. Am. Chem. Soc.* **2000**, *122*, 11138-11145.
[13] P. E. Barran, N. R. Walker, A. J. Stace, *J. Chem. Phys.* **2000**, *112*, 6173-6177.
[14] N. R. Walker, G. A. Grieves, J. B. Jaeger, R. S. Walters, M. A. Duncan, *Int. J. Mass Spectrom.* **2003**, *228*, 285.
[15] M. Adrian-Scotto, G. Mallet, D. Vasilescu, *J. Mol. Struct. (Theochem)* **2005**, *728*, 231-242.
[16] Y.-H. Zhang, M. Y. Choi, C. K. Chan, *J. Phys. Chem. A* **2004**, *108*, 1712-1718.
[17] A. Wahab, S. Mahiuddin, G. Hefter, W. Kunz, B. Minofar, P. Jungwirth, *J. Phys. Chem. B* **2005**, *109*, 24108-24120.
[18] B. Minofar, R. Vácha, A. Wahab, S. Mahiuddin, W. Kunz, P. Jungwirth, *J. Phys. Chem. B* **2006**, *110*, 15939-15944.
[19] V. Rossi, C. Sadun, L. Bencivenni, R. Caminiti, *J. Mol. Struct. (Theochem)* **1994**, *314*, 247-260.
[20] See also: K. D. Collins, *Biophys. Chem.* **2006**, *119*, 271-281.
[21] K. Nakamoto, *Infrared and Raman Spectra of Inorganic and Organometallic compounds*, 5th ed., Wiley-Interscience: New York, 1997, Part B.
[22] Calculated using the Chemputer made by M. Winter, University of Sheffield, see: http://winter.group.shef.ac.uk/chemputer/.
[23] N. Tsierkezos, D. Schröder, H. Schwarz, *J. Phys. Chem. A* **2003**, *107*, 9575-9581.
[24] J. Roithová, J. Hrušák, D. Schröder, H. Schwarz, *Inorg. Chim. Acta* **2005**, *358*, 4287-4292.
[25] J. Roithová, D. Schröder, *Angew. Chem.* **2006**, *118*, 5835-5838; *Angew. Chem. Int. Ed.* **2006**, *34*, 5705-5708.
[26] A. Andersen, F. Muntean, D. Walter, C. Rue, P. B. Armentrout, *J. Phys. Chem. A* **2000**, *104*, 692-705.
[27] M. Pavlov, P. E. M. Siegbahn, M. Sandstrom, *J. Phys. Chem. A* **1998**, *102*, 219-228.
[28] M. Alcami, A. I. Gonzalez, O. Mo, M. Yanez, *Chem. Phys. Lett.* **1999**, *307*, 244-252.
[29] For a very detailed analysis of thermal binding energies of protonated and deprotonated water clusters in a similar experimental set-up, see: Y.-S. Wang, C.-H. Tsai, Y. T. Lee, H.-C. Chang, J. C. Jiang, O. Asvany, S. Schlemmer, D. Gerlich, *J. Phys. Chem. A* **2003**, *107*, 4217-4225.
[30] Z. Sun, C.-K. Siu, O. P. Balaj, M. Gruber, V. E. Bondybey, M. K. Beyer, *Angew. Chem. Int. Ed.* **2006**, *45*, 4027-4030.
[31] D. Schröder, R. Brown, P. Schwerdtfeger, H. Schwarz, *Int. J. Mass Spectrom.* **2000**, *203*, 155-163.
[32] J. Loos, D. Schröder, W. Zummack, H. Schwarz, R. Thissen, O. Dutuit, *Int. J. Mass Spectrom.* **2002**, *214*, 105-128.
[33] C. Trage, D. Schröder, H. Schwarz, *Organometallics* **2003**, *22*, 693-707 (addendum **2003**, *22*, 1348).
[34] M. Brönstrup, D. Schröder, H. Schwarz, *Chem. Eur. J.* **1999**, *5*, 1176-1185.
[35] S. Bärsch, D. Schröder, H. Schwarz, *Chem. Eur. J.* **2000**, *6*, 1789-1796.
[36] G. K. Koyanagi, D. K. Bohme, I. Kretzschmar, D. Schröder, H. Schwarz, *J. Phys. Chem. A* **2001**, *105*, 4259-4271.
[37] D. Schröder, H. Schwarz, *Angew. Chem.* **1990**, *102*, 1466-1468; *Angew. Chem. Int. Ed. Engl.* **1990**, *29*, 1431-1433.
[38] R. Wesendrup, D. Schröder, H. Schwarz, *Angew. Chem.* **1994**, *106*, 1232-1235; *Angew. Chem. Int. Ed. Engl.* **1994**, *33*, 1174-1176.
[39] M. Brönstrup, D. Schröder, I. Kretzschmar, H. Schwarz, J. N. Harvey, *J. Am. Chem. Soc.* **2001**, *123*, 142-147.
[40] J. M. Riveros, in *Encyclopedia of Mass Spectrometry*, Vol. 1, P. B. Armentrout, Ed., Elsevier, Amsterdam, 2003, p. 262-271.
[41] L. Mac Aleese, A. Simon, T. B. McMahon. J. M. Ortega, D. Scuderi, J. Lemaire, P. Maitre, *Int. J. Mass Spectrom.* **2006**, *249*, 14-20.
[42] J. M. Ortega, F. Glotin, R. Prazeres, *Infrared Phys. Techn.* **2006**, *49*, 133-138.
[43] A. P. Scott, L. Radom, *J. Phys. Chem.* **1996**, *100*, 16502-16513.
[44] J. Zhou, G. Santambrogio, M. Brümmer, D. T. Moore, L. Wöste, G. Meijer, D. Neumark, K. R. Asmis, *J. Chem. Phys.* **2006**, *125*, 111102.
[45] M. F. Bush, R. J. Saykally, E. R. Williams, *J. Am. Chem. Soc.* **2007**, *129*, 2220-2221.
[46] J. T. Su, X. Xu, W. A. Goddard III, *J. Phys. Chem. A* **2004**, *108*, 10518-10526.
[47] D. Schröder, R. Wesendrup, R. H. Hertwig, T. Dargel, H. Graul, W. Koch, B. R. Bender, H. Schwarz, *Organometallics* **2000**, *19*, 2608-2615.

[48] G. Jancso, *Rad. Phys. Chem.* **2005**, *74*.168-171.
[49] See also: A. S. Goryunov, *Gen. Physiol. Biophys.* **2006**, *25*, 303-311.
[50] D. Schröder, T. Weiske, H. Schwarz, *Int. J. Mass Spectrom.* **2002**, *219*, 729-738.
[51] D. Schröder, M. Semialjac, H. Schwarz, *Int. J. Mass Spectrom.* **2004**, *233*, 103-109.
[52] G. Bouchoux, D. Leblanc, J. Y. Salpin, *Int. J. Mass Spectrom.* **1996**, *153*, 37-48.
[53] D. Schröder, M. Engeser, M. Brönstrup, C. Daniel, J. Spandl, H. Hartl, *Int. J. Mass Spectrom.* **2003**, *228*, 743-757.
[54] D. Schröder, H. Schwarz, S. Schenk, E. Anders, *Angew. Chem.* **2003**, *115*, 5241-5244; *Angew. Chem. Int. Ed.* **2003**, *42*, 5087-5090.
[55] D. Schröder, M. Engeser, H. Schwarz, E. C. E. Rosenthal, J. Döbler, J. Sauer, *Inorg. Chem.* **2006**, *45*, 6235-6245.
[56] D. Schröder, J. Roithová, H. Schwarz, *Int. J. Mass Spectrom.* **2006**, *254*, 197-201.
[57] B. Chiavarino, M. E. Crestoni, S. Fornarini, F. Lanucara, J. Lemaire, P. Maitre, *Angew. Chem.* **2007**, *119*, 2041-2044; *Angew. Chem. Int. Ed.* **2007**, *46*, 1995-1998.
[58] A. Simon, L. Aleese, P. Maitre, J. Lemaire, T. B. McMahon, *J. Am. Chem. Soc.* **2006**, *129*, 2829-2840
[59] S. Le Caer, Ph. D. Thesis, Université Paris-Sud, Orsay, France, 2003.
[60] D. Schröder, H. Schwarz, P. Milko, J. Roithová, *J. Phys. Chem. A* **2006**, *110*, 8346-8353.
[61] M. J. T. Frisch et al., Gaussian03, Pittsburgh PA, 2003.
[62] T. H. Dunning, Jr., *J. Chem. Phys.* **1989**, *90*, 1007-1023.